VERSITA

Chemical Papers 67 (1) 117–126 (2013)
DOI: 10.2478/s11696-012-0248-x

ORIGINAL PAPER

Effect of reactants' concentration on the ratio and yield of *E*,*Z* isomers of isatin-3-(4-phenyl)semicarbazone and *N*-methylisatin-3-(4-phenyl)semicarbazone

[a]Klaudia Jakusová*, [b]Martin Gáplovský, [a]Jana Donovalová, [a]Marek Cigáň, [a]Henrieta Stankovičová, [a]Robert Sokolík, [a]Jan Gašpar, [a]Anton Gáplovský

[a]*Institute of Chemistry, Faculty of Natural Sciences, Comenius University, Mlynská dolina CH-2, 842 15 Bratislava, Slovakia*

[b]*Department of Pharmaceutical Chemistry, Faculty of Pharmacy, Comenius University, Kalinčiakova 8, 832 32 Bratislava, Slovakia*

Received 17 April 2012; Revised 18 July 2012; Accepted 19 July 2012

Dedicated to Professor Štefan Toma on the occasion of his 75th birthday

In this work, the effect of inter- and intramolecular interactions of reactants and products, reactants concentration as well as the solvent effect on the ratio of *E* and *Z* isomers of isatin-phenylsemicarbazones in the reaction mixture is examined. Theoretical calculations proved that *Z* isomers are more stable than *E* isomers. Experimental results confirmed the noncovalent intermolecular donor-acceptor interactions of the reactants in the reaction mixture at concentrations above 0.1 mol L^{-1}. The *E*/*Z* isomer ratio of isatin-3-(4-phenyl)semicarbazone (*I*) and *N*-methylisatin-3-(4-phenyl)semicarbazone (*II*) depends on the initial concentrations of 3-amino-1-phenylurea (phenylsemicarbazide; *V*) and 1*H*-indole-2,3-dione (isatin; *III*), or 3-methylindol-2,3(1*H*)-dion (3-methylisatin; *IV*), respectively. Both isomers exhibit high thermal stability. Thermal *E*–*Z* isomerization takes place at temperatures above 70 °C in *N*,*N*-dimethylformamide.

Keywords: isatinphenylsemicarbazones, synthesis of *E*,*Z* isomers, concentration and solvent dependence, intermolecular interactions

Introduction

Considerable attention has recently been paid to the preparation of compounds which can be subjected to photoisomerization for their practical application in electronics, e.g. switches, storage media, and sensors. Inter- and intramolecular interactions, especially hydrogen bonds as relatively weak interactions, play an important role in biology; they affect, amongst other things, the course of chemical reactions and also the stability and structure of compounds. The information on their existence and their characteristics in the studied system often helps to understand the molecule's physical and chemical properties (Cubero et al., 1999; Senthilkumar et al., 2005). Formation of these hydrogen bonds often leads to hydrogen transfer from a hydroxy or amino group to the acceptor, especially in biological and photochemical processes (Levy, 1980; Li & Fang, 2003; Otsubo et al., 2002). The transfer of hydrogen (or proton) from the base or excited state of a molecule occurs in both the solution and the solid phase (Li & Fang, 2003; Alarcón et al., 1995; Falkovskaia et al., 2002; Mehata et al., 2002; Chai et al., 2005).

Inter- or intramolecular hydrogen bonds represent a very important group of interactions which affect the physico–chemical properties of compounds. The change of physico–chemical properties of chemical

*Corresponding author, e-mail: jakusova@fns.uniba.sk

compounds influences also their reactivity (Epshtein, 1979; Brancato et al., 2002). Chemical reactivity of molecules can be modified due to the change of charge density on the reaction centre after hydrogen bond stabilization/destabilization. A hydrogen bond can also lock one of the isomers or conformers (locking effect) (Kolehmainen et al., 2000) influencing thus the transition state of the chemical reaction. This specific type of noncovalent interactions consequently influences the reaction rate and the ratio of the products in the reaction mixture. Hydrogen bonds formed in compounds containing a fragment of phenylcarbazide affect the arrangement of molecules and the molecular geometry in crystals (Chai et al., 2005; Hadjoudis et al., 1999). Since photochromic properties depend on the molecule's geometry, hydrogen bonds indirectly affect also their properties (Wu et al., 2007). Additionally, bioactivity depends so strongly on the molecular conformation (molecular geometry) that the existence of intra- and intermolecular hydrogen bonds in such systems can significantly affect these processes.

Hydrazones and their derivatives, such as semicarbazones, represent a very attractive group of organic compounds. Their characteristics predispose them for practical use. An exhaustive literature review revealed that these compounds have interesting biological properties including: anti-inflammatory, analgesic, anticonvulsant, antituberculous, antitumour, anti-HIV, and antimicrobial activities (Afrasiabi et al., 2005; Sathisha et al., 2008; Verma et al., 2009; Cerchiaro & da Costa Ferreira, 2006). Synthetic versatility of hydrazone and also that of semicarbazone led to extensive use of these compounds in organic synthesis. They are often used in the synthesis of heterocyclic compounds (Verma et al., 2004; Farghaly et al., 2009; Sridhar et al., 2001; Pandeya et al., 2000, 2002, 2006; Pal et al., 2011; Dimmock et al., 2000; Sonawane et al., 2009; Jafri et al., 2012). Wide practical application of hydrazones and their derivatives also encouraged the study of azo–hydrazone tautomeric equilibrium and *E*–*Z* isomerization of these compounds. Influence of the molecular structure, temperature, and solvent on these equilibriums was thus investigated.

In this study, the synthesis of *E* and *Z* isomers of *I* and *II*, and the ability of reactants' concentration and solvent to affect the ratio of these isomers in the reaction mixture during their synthesis from 1*H*-indole-2,3-dione (isatin; *III*) (or 3-methylindol-2,3(1*H*)-dione (3-methylisatin (*IV*), respectively), and 3-amino-1-phenylurea (phenylsemicarbazide; *V*) were investigated.

Experimental

Materials and methods

Melting points (uncorrected) were measured on a Kofler hot stage (Nagema, Germany). ^{1}H NMR spectra were recorded at 300 MHz on a Varian Gemini 200 spectrometer (Varian, USA) using $CDCl_3$ or DMSO-d_6 as solvents and trimethylsilane as an internal standard. Chemical shifts are given in δ related to the internal standard. IR spectra were recorded on a spectrometer Nicolet FT-IR 6700 (Nicolet, USA). UV spectra were measured on an Agilent 8543 (Agilent Technologies, USA). Elemental analyses were performed on a Carlo Erba Strumentacione 1106 apparatus (Carlo Erba Strumentacione, Italy).

HPLC chromatography was carried out using a chromatographic system (Agilent Technologies, USA) consisting of a quaternary pump, thermostated column compartment, a diode array detector (VWDG 1314A), manual injector (Rheodyne model 7725i) with 20 μL sample loop, and a degasser (g1379A) all of the 1100 series. For all experiments, Column ZORBAX-SB-Phenyl (150 mm × 4.6 mm i.d.) was used. For analyses of *I*, mobile phase A was a methanol/water mixture ($\varphi_r = 1 : 99$) and phase B was acetonitrile. In the analysis of isomers, the isocratic gradient A/B ($\varphi_r = 1 : 1$) at the flow rate of 0.6 mL min^{-1} at 22 ℃ and detection at 236 nm was used. The injection volume was 20 μL. For analyses of *II*, mobile phase A was a methanol/water mixture ($\varphi_r = 1 : 99$) and phase B was methanol. In the analysis of isomers, the isocratic gradient A/B ($\varphi_r = 37 : 13$) at the flow rate of 0.6 mL min^{-1} at 22 ℃ and detection at 236 nm was used. The injection volume was 20 μL.

Chemicals and solvents were purchased from the major chemical suppliers. EtOH, MeOH, $CHCl_3$, and DMF from Merck (Germany), 3-methylisatin (*IV*) from Acros Organics (Belgium), isatin (*III*), phenylsemicarbazide (*V*), and $KClO_4$ from Sigma–Aldrich (USA) as the highest purity grade. Deionized water for HPLC analysis was purified by a Pro-PS water purification system (Labconco, USA) and subsequently purified by Simplicity (Millipore, France). Unless otherwise noted, all materials were used as received without further purification. All solvents were dried by standard methods and distilled prior to use. All reactions were performed using oven-dried glassware. Reactions were monitored using Merck analytical thin layer chromatography (TLC) plates (silica gel 60 F_{254}; Merck, Germany) with eluent (hexane/ethyl acetate $\varphi_r = 1 : 1$) and analyzed with 254 nm UV light. For column chromatography, Silica gel 60 (Merck, 230-400 mesh ASTM, Merck, Germany) with indicated solvent was used.

Characterization of E and Z isomers of I and II

A solution of *V* (6 mmol) in hot absolute ethanol (20 mL) was added to *III* or *IV* (6 mmol) in hot absolute ethanol (130 mL). The reaction mixture was refluxed for 2 h and the formed precipitate (*Ia*; *E* isomer) was filtered off from the hot solution, washed

Table 1. Characterization data of prepared compounds *Ia*, *Ib*, *IIa*, and *IIb*

Compound	Formula	M_r	w_i(calc.)/% w_i(found)/%			Yield	M.p.
			C	H	N	%	℃
Ia	$C_{15}H_{12}N_4O_2$	280.28	64.28	4.32	19.99	54	193–196
			64.15	4.35	19.78		
Ib	$C_{15}H_{12}N_4O_2$	280.28	64.28	4.32	19.99	45	210–213
			64.26	4.19	19.82		
IIa	$C_{16}H_{14}N_4O_2$	294.31	65.30	4.79	19.04	59	170–172
			65.28	4.47	18.81		
IIb	$C_{16}H_{14}N_4O_2$	294.31	65.30	4.79	19.04	40	198–201
			65.32	4.52	18.95		

Table 2. Spectral data of *Ia*, *Ib*, *IIa*, and *IIb*

Compound	Spectral data
Ia	IR ($CHCl_3$) $\tilde{\nu}$/cm^{-1}: 1448 (C═N), 1536 (C═C), 1602 (C═O), 1735 (C═O), 3380 (N—H), 3442 (N—H) ^{1}H NMR (DMSO-d$_6$), δ: 6.91–6.93 (d, 1H, J = 7.8 Hz, Ar-H), 7.04–7.12 (m, 2H, Ar-H), 7.32–7.41 (m, 3H, Ar-H), 7.58 (dd, 2H, J = 8.7 Hz, J = 1.2 Hz, Ar-H), 8.09 (d, 1H, J = 7.5 Hz, Ar-H), 9.49 (s, 1H, NH), 10.39 (s, 1H, NH), 10.76 (s, 1H, NH)
Ib	IR ($CHCl_3$) $\tilde{\nu}$/cm^{-1}: 1448 (C═N), 1533 (C═C), 1621 (C═O), 1706 (C═O), 3255 (N—H) ^{1}H NMR (DMSO-d_6), δ: 6.94 (d, 1H, J = 7.8 Hz, Ar-H), 7.04–7.13 (m, 2H, Ar-H), 7.31–7.37 (m, 3H, Ar-H), 7.61–7.64 (m, 2H, Ar-H), 7.67 (d, 1H, J = 6.9 Hz, Ar-H), 9.84 (s, 1H, NH), 11.99 (s, 1H, NH), 12.25 (s, 1H, NH)
IIa	IR ($CHCl_3$) $\tilde{\nu}$/cm^{-1}: 1448 (C═N), 1535 (C═C), 1604 (C═O), 1716 (C═O), 3380 (N—H) ^{1}H NMR ($CDCl_3$), δ: 3.30 (s, 3H, CH_3), 6.93 (d, 1H, J = 3.9 Hz, Ar-H), 7.10–7.15 (m, 2H, Ar-H), 7.34–7.37 (m, 2H, Ar-H), 7.44–7.47 (ddd, 1H, J = 3.9 Hz, J = 0.6 Hz, J = 0.3 Hz, Ar-H), 7.61 (dd, 2H, J = 4.5 Hz, J = 0.6 Hz, Ar-H), 7.79 (d, 1H, J = 3.9 Hz, Ar-H), 8.79 (s, 1H, NH), 9.10 (s, 1H, NH)
IIb	IR ($CHCl_3$) $\tilde{\nu}$/cm^{-1}: 1448 (C═N), 1533 (C═C), 1617 (C═O), 1691 (C═O), 3249 (N—H), 3394 (N—H) ^{1}H NMR ($CDCl_3$), δ: 3.30 (s, 3H, CH_3), 6.90–6.93 (d, 1H, J = 7.8 Hz, ArH), 7.10–7.19 (m, 2H, Ar-H), 7.34–7.44 (m, 3H, Ar-H), 7.58–7.66 (m, 3H, Ar-H), 8.31 (s, 1H, NH), 12.09 (s, 1H, NH)

with ethanol and dried. *Z* isomer of *I* (*Ib*) was isolated and purified by column chromatography using silica gel as the stationary phase, hexol (a mixture of methylpentanes and hexane; $\varphi_r \approx 2:1$)/ethyl acetate ($\varphi_r = 1:1$) as the mobile phase. Isomers *IIa* (*E* isomer) and *IIb* (*Z* isomer) were isolated from the evaporated reaction mixture and purified using the same method as for *Ib*. Experimental yields and spectral data of *Ia*, *Ib*, *IIa*, and *IIb* are summarized in Tables 1 and 2.

Although *I* is not a new compound (Borsche & Meyer, 1921; Kang et al., 2011), its isolation or a more detailed study of *Ib* and the noncovalent interactions of both isomers have not been performed until now (to the best of our knowledge).

General procedure for the synthesis of I and II (HPLC analysis)

HPLC analysis was used for the determination of the ratio of *E*/Z isomers in the reaction mixture in various solvents. A solution of *V* (0.1 mol L^{-1}, 0.01 mol L^{-1}, or 0.001 mol L^{-1}) in different solvents (15 mL) was mixed with the solutions of *III* or *IV* (0.1 mol L^{-1}, 0.01 mol L^{-1}, or 0.001 mol L^{-1}) in the corresponding solvent (10 mL). The reaction mixture was refluxed for 3 h in EtOH, EtOH + $KClO_4$ (5 mass %), and $CHCl_3$; in *N*,*N*-dimethylformamide (DMF), the reaction mixture was tempered at 50 ℃ (due to the back isomerization of *Z* isomers). Experimental yields are summarized in Tables 3 and 4.

Quantum-chemical calculations

The quantum-chemical calculations were performed on the B3LYP/6-31G+(d,p) level of theory for isatinphenylsemicarbazone isomers and the M062X/6-31+G(d,p) level of theory was applied for the reactants configurations as it includes the dispersion term for better treatment of noncovalent interactions (Zhao & Truhlar, 2008). The calculations were performed using the Gaussian version 03 (Gaussian, USA) and the Jaguar version 7.7 (Schrödinger, USA), respectively. The local energy minima were confirmed by vibrational analysis of all structures.

Table 3. Overall and individual yields of the reaction of *IV* with *V*

N-methylisatin												
c/(mol L^{-1})	EtOH			EtOH + $KClO_4^a$			$CHCl_3$			DMF^b		
	Y_{E+Z}/%	Y_E/%	Y_Z/%	Y_{E+Z}/%	Y_E/%	Y_Z/%	Y_{E+Z}/%	Y_E/%	Y_Z/%	Y_{E+Z}/%	Y_E/%	Y_Z/%
0.1	58.9	59.4	40.6	76.3	76.7	23.3	90.3	84.4	15.6	1.0	89.4	10.6
0.01	39.9	72.9	27.1	71.8	72.9	15.6	87.9	85.9	14.1	0.2	55.5	44.5
0.001	32.7	75.2	24.8	72.4	75.2	13.0	83.3	88.1	11.9	0.4	16.9	83.1

a) 5 mass % of $KClO_4$; *b*) At 50 °C; c – initial concentration of reactants; Y_{E+Z} – overall yield of both (E + Z) isomers; Y_E – yield of E isomer, Y_Z – yield of Z isomer.

Table 4. Overall and individual yields of the reaction of *III* with *V*

Isatin												
c/(mol L^{-1})	EtOH			EtOH + $KClO_4^a$			$CHCl_3$			DMF^a		
	Y_{E+Z}/%	Y_E/%	Y_Z/%	Y_{E+Z}/%	Y_E/%	Y_Z/%	Y_{E+Z}/%	Y_E/%	Y_Z/%	Y_{E+Z}/%	Y_E/%	Y_Z/%
0.1	94.8	54.4	45.7	51.6	76.4	23.6	66.5	87.0	13.0	95.6	90.1	9.9
0.01	54.7	77.7	22.3	22.1	80.1	19.9	30.7	87.2	12.8	41.6	90.4	9.6
0.001	14.3	89.5	10.5	16.0	89.7	10.3	16.0	95.2	4.8	30.3	90.2	9.8

a) 5 mass % of $KClO_4$; c – initial concentration of reactants; Y_{E+Z} – overall yield of both (E + Z) isomers; Y_E – yield of E isomer, Y_Z – yield of Z isomer.

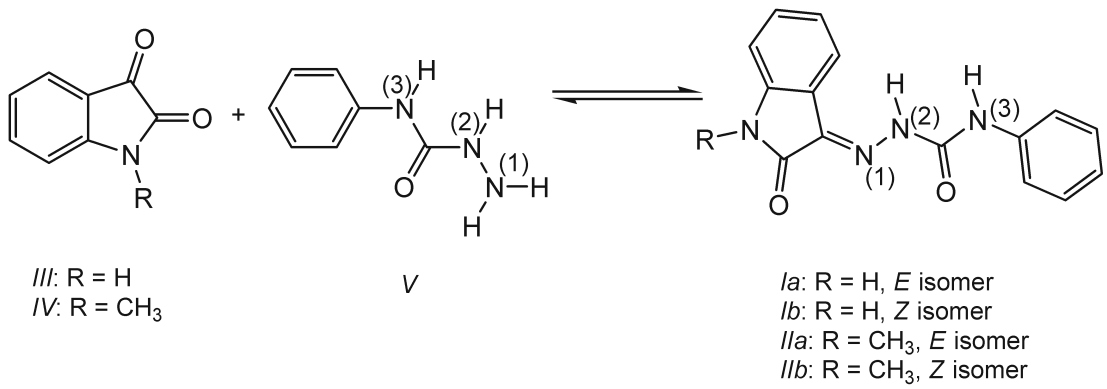

Fig. 1. Synthesis of *I* and *II* in different solvents ($CHCl_3$, EtOH, EtOH + $KClO_4$, or DMF).

Results and discussion

Under conditions often used in the preparation of isatinsemicarbazones derivatives via the condensation of 1*H*-indole-2,3-dione (isatin) derivatives and carbazides (Pandeya et al., 2002), the less soluble product, here the less soluble geometric isomer, is directly isolated by filtration from the reaction mixture. Depending on the thermodynamic stability of the isolated isomer of *I* (isatin-3-(4-phenyl)semicarbazone) and *II* (*N*-methylisatin-3-(4-phenyl)semicarbazone), respectively, a thermally or photochemically initiated isomerization can occur after its re-dissolution. Isomerization is completed after reaching the equilibrium. Due to the practical applications of these compounds, it is important to understand the formation mechanism of *E* or *Z* isomers and their stabilities. This is necessary because other isomers can also be formed, and their properties may not be suitable for the required application.

I and *II* and their *E* and *Z* isomers were prepared by the reaction of isatin (*III*) or methylisatin (*IV*) with phenylsemicarbazide (*V*), as shown in Fig. 1.

The reactions were carried out in chloroform, ethanol, ethanol + $KClO_4$, and DMF. UV-VIS spectra of *E* and *Z* isomers of *I* and *II* in methanol are shown in Fig. 2.

UV-VIS absorption spectra of *E* isomers of both compounds, *I* and *II*, exhibit long-wavelength absorption bands located at 410 nm and 326 nm, respectively, and a shoulder containing short-wavelength bands with the maximum at 240 nm. The shapes

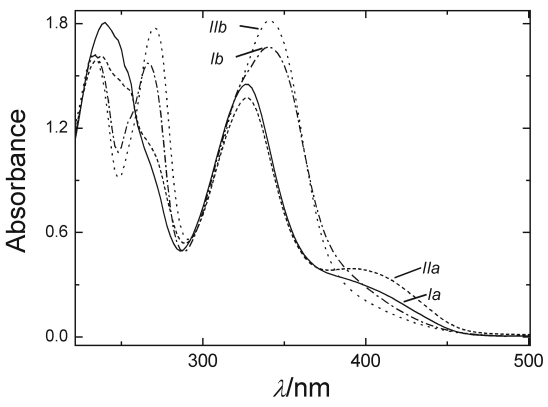

Fig. 2. UV-VIS spectra of compounds *Ia*, *Ib*, *IIa*, and *IIb* in MeOH (concentration of 10^{-4} mol L^{-1}).

and positions of the absorption maxima in the spectra are identical. They differ only in the extinction coefficients; *IIa* has higher extinction coefficient at 410 nm (3535 L mol^{-1} cm^{-1}) compared to *I* (2533 L mol^{-1} cm^{-1}). At shorter wavelengths (326 nm and 240 nm), the extinction coefficients of methyl derivative *IIa* are lower (13722 L mol^{-1} cm^{-1} and 15959 L mol^{-1} cm^{-1}, respectively) compared to those of *Ia* (14519 L mol^{-1} cm^{-1} and 18069 L mol^{-1} cm^{-1}, respectively).

Z isomers of *I* and *II* have absorption maxima at 342 nm (16617 L mol^{-1} cm^{-1} and 18154 L mol^{-1} cm^{-1}, respectively), 271 nm (14475 L mol^{-1} cm^{-1} and 17665 L mol^{-1} cm^{-1}, respectively), and 232 nm (16121 L mol^{-1} cm^{-1} and 16304 L mol^{-1} cm^{-1}, respectively). The absorption maximum located at 326 nm in the spectra of *E* isomers is more bathochromically shifted for *Z* isomers ($\approx$ 24 nm). The methyl substituent does not affect the position of the absorption maxima. Instead of one complex absorption band at 240 nm noted in the spectra of *E* isomers, there are two well resolved absorption bands with maxima at 271 nm and 232 nm in the *Z* isomers' spectra. The absorption maximum for the *Z* isomer of *II* at 271 nm is bathochromically shifted by approximately 4 nm compared to that for the *Z* isomer of the non-methylated isatine derivative *I*. The increasing polarity of the solvent (chloroform–methanol exchange) leads to a small bathochromic shift of the absorption band of *E* isomers at 326 nm ($\approx$ 4 nm), and to a hypsochromic shift of the absorption band of *Z* isomers located at approximately 342 nm ($\approx$ 5 nm). Methanol as a polar protic solvent disturbs the intramolecular hydrogen bond in *Z* isomers, which leads to a hypsochromic shift of the absorption maxima.

If the reaction is not affected by other factors (except for the stability of isomers), the reaction mixture should contain only the more stable isomer, or at least a very high percentage of it. According to the bathochromic shift in the UV-VIS spectra, higher intensity of the absorption band at 342 nm and IR spectra for these isomers indicates that *Z* isomers are more stable than *E* isomers. The slightly increased stability of *Z* isomers was confirmed by the quantum-chemical calculations using the Gaussian 03 program. Geometry optimization and frequency calculation of the *E* and *Z* isomers were done at the B3LYP/6-31+G(d,p) level of theory. *Z* isomers were found to be more stable than *E* isomers by approximately 19.9 kJ mol^{-1} for *IIb* and 18.8 kJ mol^{-1} for *Ib*, respectively. The intramolecular hydrogen bonds significantly contribute to the higher stability of *Z* isomers compared to *E* isomers (Fig. 3).

Experimental results show that the stability of the isomers of derivatives *I* and *II* is not the only factor affecting their ratio in the reaction mixture.

Data in Tables 3 and 4 indicate that the overall yield of *I* and *II* depends on the initial concentration of the reactants and on the type of the solvent. The effect of these factors on the overall yield varies depending on the reaction partner of *V* is *III* or *IV*. If *III* is the reactant in this condensation reaction, the highest overall yield is achieved at the highest concentration of the reactants in all solvents. The overall yield decreases with the decreasing concentration of the reactants and reaches approximately 16 %, except for DMF at the concentration of 10^{-3} M. In the reaction of *IV* with *V*, the same trend on the overall yield of products as for *III* was observed. The concentration

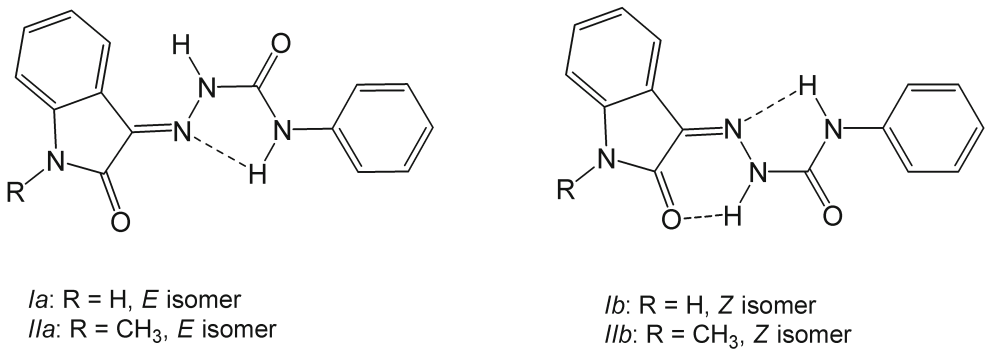

Fig. 3. Intramolecular hydrogen bonding in *E* and *Z* isomers of compounds *I* and *II*.

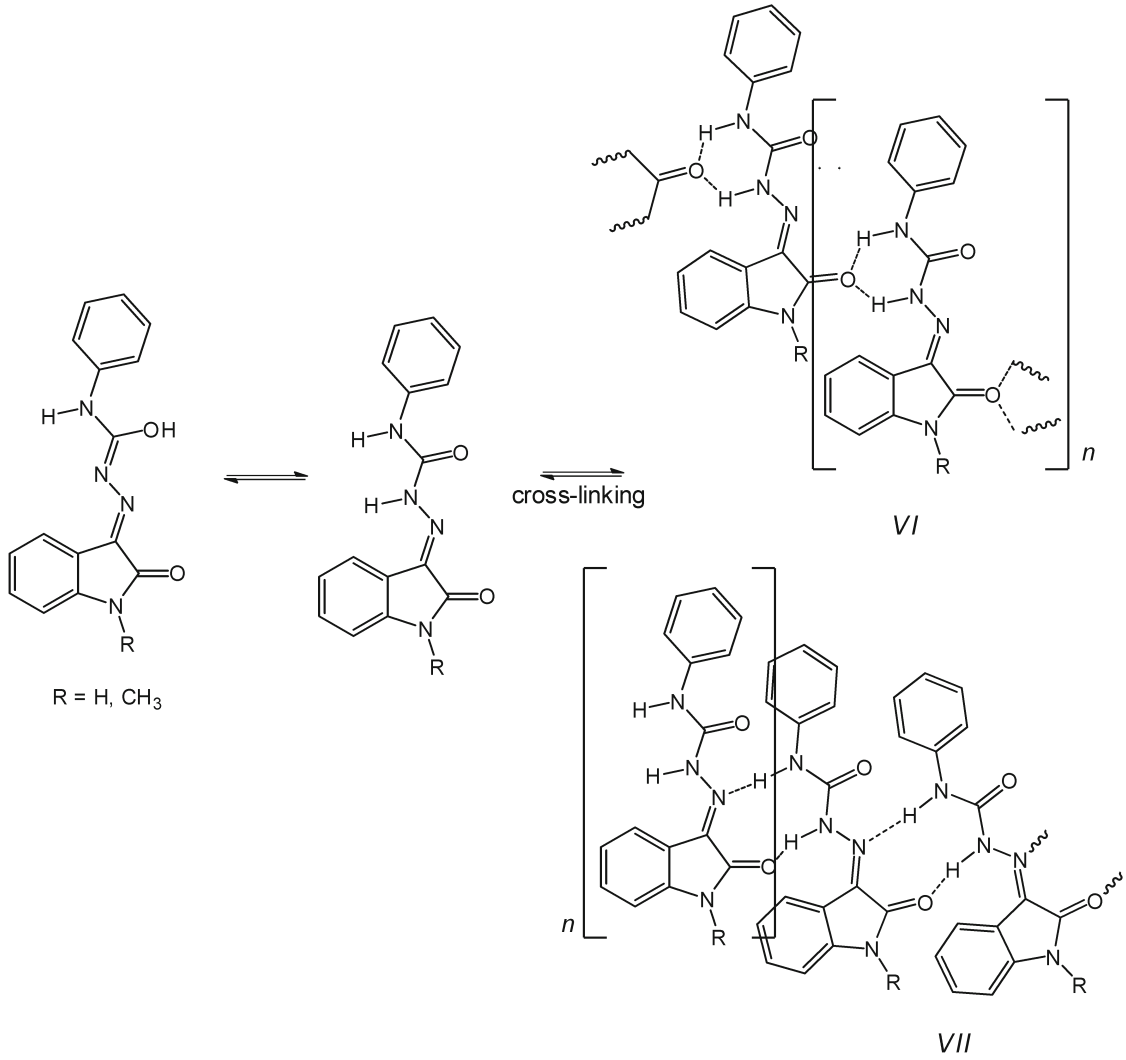

Fig. 4. Possible noncovalent intermolecular interactions between molecules of derivatives *I* and *II*.

of reactants also affects the overall yield of the isomers; however, this yield is in case of *IV* less dependent on the initial concentration of reactants in comparison to *III*. The overall yields are very low (< 1 %) and practically independent of the initial concentration of reactants for the reaction of *IV* in DMF.

Thermodynamic stability of both isomers of *I* and *II* is one of the parameters that can substantially affect the ratio of the isomers in the reaction mixture. Depending on the thermodynamic stability and on the reaction conditions, the change from one isomer to the other one occurs in the subsequent reaction. Therefore, this problem was addressed by studying the effect of temperature and solvent polarity on the isomerization of *E* and *Z* isomers of *I* and *II*, respectively. Both *E* and *Z* isomers are stable at the concentration of 10^{-4} mol L^{-1} in ethanol and chloroform at 55 ℃ or 65 ℃. UV-VIS spectra of *E* isomers in ethanol at 65 ℃ showed only a very small change in the absorbance value at 326 nm. This change in the spectrum is not caused by the geometric *E*–*Z* isomerization. We were unable to prove the presence of *Z* isomers using UV-VIS, IR, or NMR spectra. Similar behavior of *E* isomers was observed in DMF at 50 ℃. This change in the spectrum can be attributed to the alteration in the molecule's geometry as a result of intermolecular interactions. This statement is based on the fact that the scale of this change and its rate are proportional to the concentration of *I* and *II*. Some possible intermolecular interactions of derivatives *I* and *II* are shown in Fig. 4.

An increase in the concentration shifts the equilibrium to the right, which results in the formation of a supramolecule. From structures depicted in Fig. 4, structure *VI* is more feasible because this interaction results in a six-membered ring which can share six electrons localized on the heteroatoms providing conditions for the existence of a quasi-aromatic system. The higher stability of this structure in DMF is caused by the high dielectric constant of the solvent. On the contrary, proton–donor solvents, such as ethanol, reduce the strength of hydrogen bonds in the

Table 5. Rate constants k_1 and k_2 of product *II* (DMF, $T = 100\,℃$)

$c \cdot 10^{-3}/(\text{mol L}^{-1})$	$k_1 \cdot 10^{-3}/\text{s}^{-1}$	$k_2 \cdot 10^{-3}/\text{s}^{-1}$
0.1	0.9564	0.44
0.02	1.0700	0.054
0.05	1.1300	0.026

c – Initial concentration of reactants ($c = c_{IV} = c_V$; where c_{IV} is the concentration of *IV* and c_V is the concentration of *V*); k_1 – rate constants of the breakdown of the supramolecule aggregate; k_2 – rate constant of the formation of the *Z* isomer of isatinsemicarbazone *II* (*IIb*).

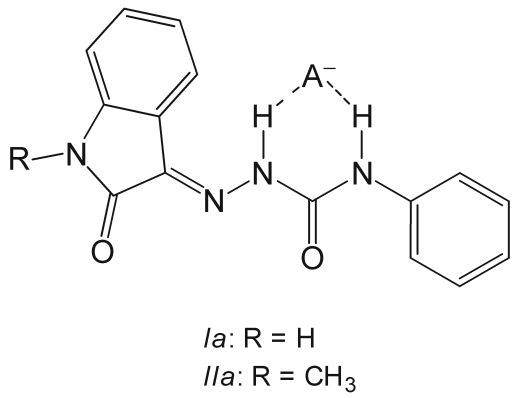

Fig. 5. Possible noncovalent intermolecular interactions of derivatives *Ia* and *IIa* with ClO_4^- (A^-).

supramolecule and its structure becomes less stable compared to that achieved in DMF. This explanation is consistent with the experimental results verifying the stability of *I* and *II* in DMF at 100 ℃. In the initial phase of the reaction (at all initial concentrations) under the studied conditions, a decrease in the absorbance was observed at 326 nm in the UV-VIS spectra of *E* isomers (Table 5). However, no *Z* isomers in the solution were detected. After approximately half an hour, an increase in the absorbance at 342 nm characteristic for *Z* isomers was observed, during this second phase of the reaction (Table 5). The presence of *Z* isomers in the solution was confirmed by both NMR and FTIR spectroscopy. The scale of the changes in the UV-VIS spectrum (absorbance at 326 nm) and also the rates of the changes depend on the initial concentrations of *I* and *II*. At low concentrations of *I* and *II*, the abundance of "supramolecules" is limited and therefore it is not possible to observe the first phase of the reaction in the UV-VIS spectra. Accordingly, the effect of $KClO_4$ on the stability of *I* and *II* and on the ratio of their *E* and *Z* isomers in ethanol can be explained by the interaction of the ClO_4^- anion (A^-) with the *I* and *II* molecules (Fig. 5).

This interaction increases the conjugation and thereby also the stability of the isomers (Jia et al., 2010); on the other hand, the fact that under heterogeneous conditions molecules of *I* and *II* are fixed on the surface of $KClO_4$ plays a significant role. A similar interaction with the ClO_4^- anion can also be expected for *V*, explaining thus the almost independent concentration of *E* isomers in the reaction mixture of ethanol

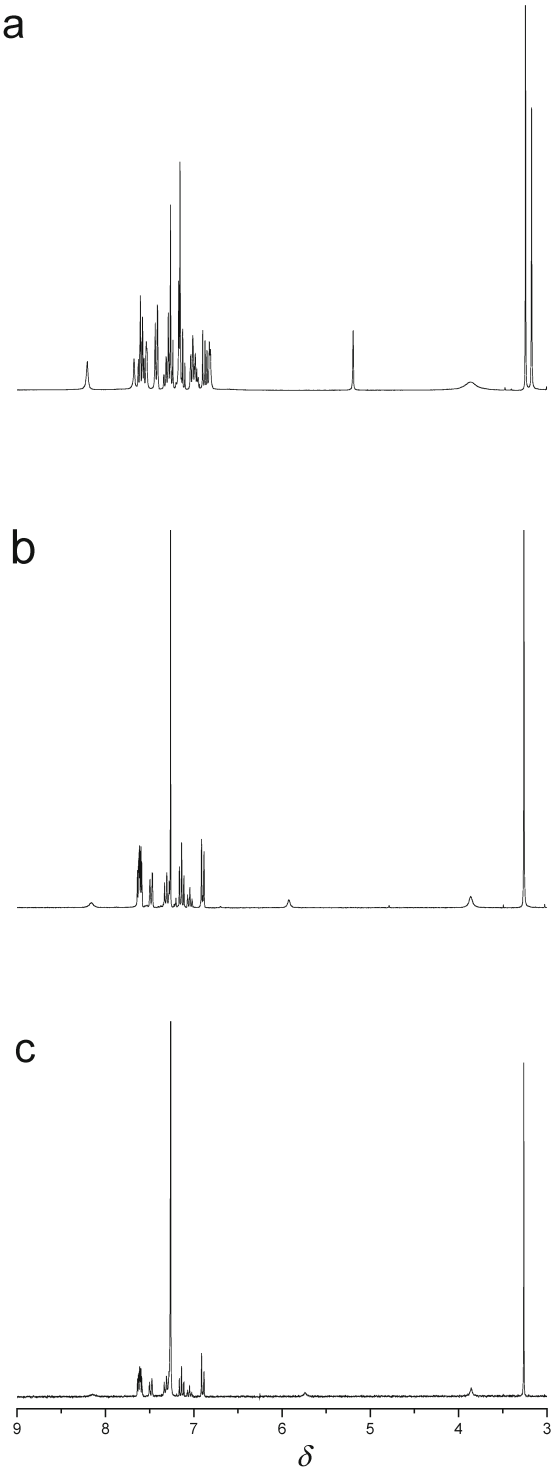

Fig. 6. ^{1}H NMR spectrum of the mixture (mole ratio, 1 : 1) of *IV* a *V* in $CDCl_3$ at $t = 0$ s, $T = 20\,℃$; $c_{IV} = c_V = 10^{-1}$ mol L^{-1} (a); $c_{IV} = c_V = 10^{-2}$ mol L^{-1} (b); $c_{IV} = c_V = 10^{-3}$ mol L^{-1} (c).

Table 6. Dependence of the shift in the ^{1}H NMR spectrum for hydrogens attached to nitrogen on the concentration of reactants

c/(mol L^{-1})	Compound								
	V			*III*	*IV*	Mixture of *IV* and *V* (mole ratio, 1 : 1)			
	$\delta_{N(1)}$	$\delta_{N(2)}$	$\delta_{N(3)}$	δ_H	δ_{CH3}	$\delta_{N(1)}$	$\delta_{N(2)}$	$\delta_{N(3)}$	δ_{CH3}
0.1	3.818	6.687	8.200	8.178	3.261	3.158	5.253	8.201	3.235
0.01	3.854	6.086	8.169	7.915	3.262	3.856	6.057	8.157	3.259
0.001	3.858	5.750	8.140	7.607	3.262	3.859	5.755	8.140	3.261

c – Initial concentration of the corresponding compound; $\delta_{N(1)}$ – chemical shift for hydrogens attached to nitrogen N-1 of *V*, $\delta_{N(2)}$ – chemical shift for hydrogens attached to nitrogen N-2 of *V*, $\delta_{N(3)}$ – chemical shift for hydrogens attached to nitrogen N-3 of *V*, δ_H – shift for hydrogens attached to nitrogen of *III*, δ_{CH3} – shift for CH_3 hydrogens attached to nitrogen of *IV*.

+ $KClO_4$, with regard to the initial reactant concentrations.

The existence of the preliminary tautomeric equilibrium of reactants (Fig. 4), where the equilibrium constants vary due to the intermolecular interactions between the reactants themselves and between the reactants and the molecules of the solvent, can also affect the ratio of *E* and *Z* isomers in the reaction of *III* or *IV* with *V*. Intermolecular interactions induce (even prior to the formation of a transition state) the arrangement of reactants ensuring the preference to the formation of one isomer in the transition state and thus affecting the ratio of the *E* and *Z* isomers in the reaction mixture.

We were unable to clearly demonstrate the precise intermolecular interactions between *V* and *III* or *IV* by UV-VIS and FTIR spectroscopy. The effect of the reactants' concentration on the position and intensity of signals for hydrogens of the aromatic ring, those attached to nitrogens and those of the methyl group in the ^{1}H NMR spectrum of the mixture of *IV* a *V*, is shown in Fig. 6. Chemical shifts of the signals for hydrogens of the methyl group of isatin and also for the change of the signals for all aromatic hydrogens of both reactants were clearly evident at the 10^{-1} M concentration of reactants. The dependence of the shift in hydrogens attached to nitrogen on the concentration of reactants is shown in Table 6.

^{1}H NMR spectrum of *IV* alone does not change with its concentration. The change of the chemical shifts for hydrogens attached to nitrogens of *III* and *V* with the concentration of *III* (Table 6) indicates the existence of intermolecular hydrogen bonds between the molecules of *III* and *V*. The dependence of the intensity of ^{1}H NMR signals on the temperature (Fig. 7) proves that the shift of the NMR signals (Fig. 6) is caused by the existence of the chemical equilibrium between noncovalently bound *IV* with *V* and noninteracting molecules *IV* and *V*. Data from the ^{1}H NMR spectra confirmed the existence of noncovalent intermolecular interactions of type *III*-*III*, *IV*-*IV*, *V*-*V*, *III*-*V*, and *IV*-*V* in the reaction system. The concentration of noninteracting reactants in the reaction system, the equilibrium state, depends on the type of

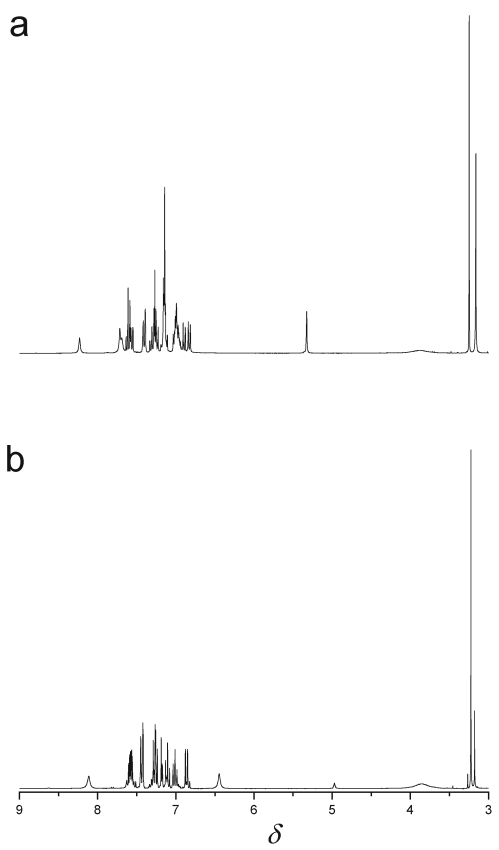

Fig. 7. ^{1}H-NMR spectrum of the mixture (mole ratio, 1 : 1) of *IV* a *V* in $CDCl_3$ at $t = 0$ s; $T = 10$ °C (a); $T = 50$ °C (b).

the solvent, temperature, concentration of reactants, and it is probably a factor which significantly affects the ratio of *E* and *Z* isomers of *I* and *II* in the reaction of *III* or *IV*, respectively, with *V*.

These experimental findings support the results of the performed calculations (Fig. 8, Table 7). Fig. 8 demonstrates the optimized geometry for the most significant reactant configurations of *IV* and *V* found at the M062X/6-31+G(d,p) level of theory.

Results of the calculations (Fig. 8, Table 7) and changes of the shifts in the ^{1}H NMR spectrum for

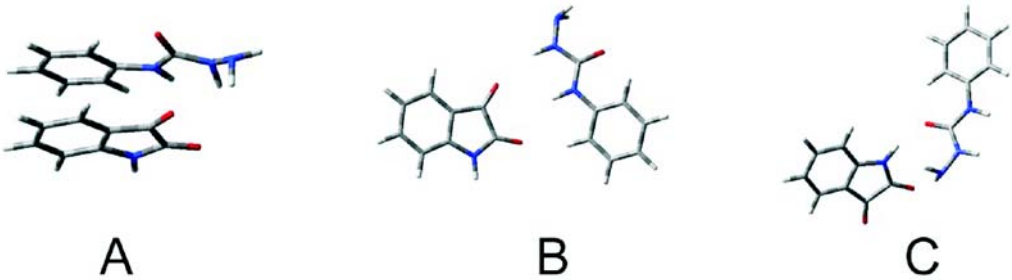

Fig. 8. Optimized geometry for the most significant reactant configurations A, B, and C of *IV* and *V* found at the M062X/6-31+G(d,p) level of theory; carbon – grey , hydrogen – white, nitrogen – blue, oxygen – red.

Table 7. M062X/6-31+G(d,p) optimized geometries for the three lowest energy reactant configurations A, B, and C of *IV* and *V*

Reactant geometry	ΔG/(kJ mol^{-1})
A	0.0
B	4.8^a
C	4.9^a

a) Geometry contains one weak negative frequency; ΔG – Gibbs energy for the three lowest energy reactant configurations A, B, and C of *IV* and *V* found at the M062X/6-31+G(d,p) level of theory.

hydrogens of the reactants show a preference for the donor–acceptor interaction in configuration A. This interaction takes place over a space where *III* or *IV* acts as the acceptor and *V* as the donor. Such arrangement of the reactants favors the formation of *E* isomers rather than of *Z* isomers. This conclusion is based on the assumption that it is necessary to stabilize the transition state, and consequently also the product, by inter- and intramolecular interactions to achieve the formation of the less stable *E* isomers. The ratio of *E* and *Z* isomers of *I* and *II* in ethanol in the presence of $KClO_4$ confirmed this assumption. Based on these findings, it is impossible to definitely state which configuration of the reactants leads to the preferential formation of *Z* isomers, or indeed, if any configuration does. Access of *V* to the reaction centre of *III* is spatially unlimited for noninteracting reactants, in terms of noncovalent intermolecular interactions. Therefore, formation of *Z* isomers from noninteracting reactants is quite possible since *Z* isomers are more stable than *E* isomers.

Conclusions

The overall yield of isatin-3-(4-phenyl)semicarbazone (*I*) and *N*-methylisatin-3-(4-phenyl)semicarbazone (*II*) formation process depends on the initial concentration of the reactants and on the type of the solvent. The effect of these factors on the overall yield varies depending on the reaction partner of phenylcarbazide is isatin or *N*-methylisatin. The reaction with isatin in all employed solvents provides the highest yield at the highest initial concentration of the reactants; this yield decreases with the decreasing reactants' concentration. Similarly, the ratio of *E* and *Z* isomers in the reaction mixture depends on the solvent and on the initial concentration of the reactants. This dependence is related with the intermolecular interactions between the reactants (inducing mutual arrangement of the reactants ensuring the preference to the formation of one isomer in the transition state) and intermolecular interactions between the molecules of the product (affecting the stability of both isomers). *E* and *Z* isomers of isatin-3-(4-phenyl)semicarbazone and *N*-methylisatin-3-(4-phenyl)semicarbazone are stable up to 70 ℃. Increasing the temperature above 70 ℃ causes thermal *E*–*Z* isomerization. Under these conditions, the equilibrium related to noncovalent intermolecular interactions overtakes the following *E*–*Z* isomerization. The range of this preliminary equilibrium depends on the initial concentration of the reactants. ^{1}H NMR spectra confirmed the existence of noncovalent intermolecular interactions between the reactants, and the experimental results are consistent with the quantum-chemical calculations.

Acknowledgements. This work was supported by the Slovak Grant Agency for Science (Grant No. 1/1126/11).

References

Afrasiabi, Z., Sinn, E., Lin, W., Ma, Y., Campana, C., & Padhye, S. (2005). Nickel (II) complexes of naphthaquinone thiosemicarbazone and semicarbazone: Synthesis, structure, spectroscopy, and biological activity. *Journal of Inorganic Biochemystry*, *99*, 1526–1531. DOI: 10.1016/j.jinorgbio.2005.04.012.

Alarcón, S. H., Olivieri, A. C., Labadie, G. R., Cravero, R. M., & González-Sierra, M. (1995). Tautomerism of representative aromatic α-hydroxy carbaldehyde anils as studied by spectroscopic methods and AM1 calculations. Synthesis of 10-hydroxyphenanthrene-9-carbaldehyde. *Tetrahedron*, *51*, 4619–4626. DOI: 10.1016/0040-4020(95)00002-p.

Borsche, W., & Meyer, R. (1921). Über Desoxy-indigo. *Berichte der Deutschen Chemischen Gesellschaft (A and B Series)*, *54*, 2854–2856. DOI: 10.1002/cber.19210541037.

Brancato, G., Coutrot, F., Leigh, D. A., Murphy, A., Wong, J. K. Y., & Zerbetto, F. (2002). From reactants to products

via simple hydrogen-bonding networks: Information transmission in chemical reactions. *PNAS*, *99*, 4967–4971. DOI: 10.1073/pnas.072695799.

Cerchiaro, G., & da Costa Ferreira, A. M. (2006). Oxindoles and copper complexes with oxindole-derivatives as potential pharmacological agents. *Journal of the Brazilian Chemical Society*, *17*, 1473–1485. DOI: 10.1590/s0103-50532006000800003.

Chai, H., Liu, G., Liu, L., Jia, D., Guo, Z., & Lang, J. (2005). Crystal structure and spectroscopic study on photochromism of 1,3-diphenyl-4-(4'-fluoro)benzal-5-pyrazolone N(4)-phenyl semicarbazone. *Journal of Molecular Structure*, *752*, 124–129. DOI: 10.1016/j.molstruc.2005.04.047.

Cubero, E., Orozco, M., Hobza, P., & Luque, J. F. (1999). Hydrogen bond versus anti-hydrogen bond: A comparative analysis based on the electron density topology. *Journal of Physical Chemistry A*, *103*, 6394–6401. DOI: 10.1021/jp990258f.

Dimmock, J. R., Vashishtha, S. C., & Stables, J. P. (2000). Urelylene anticonvulants and related compounds. *Pharmazie*, *55*, 490–494.

Epshtein, L. M. (1979). Hydrogen bonds and the reactivity of organic compounds in proton transfer and nucleophilic substitution reactions. *Russian Chemical Reviews*, *48*, 854–867. DOI: 10.1070/rc1979v048n09abeh002417.

Falkovskaia, E., Pivovarenko, V. G., & del Valle, J. C. (2002). Observation of a single proton transfer fluorescence in a biaxially symmetric dihydroxy diflavonol. *Chemical Physics Letters*, *352*, 415–420. DOI: 10.1016/s0009-2614(01)01490-7.

Farghaly, M., Abbel-Wahab, B. F., & Ahmed, E. M. (2009). Synthesis, antiviral and antimicrobial screening of some new 2-oxoindoline derivatives. *Chemistry of Heterocyclic Compounds*, *45*, 539–544. DOI: 10.1155/2008/362105.

Hadjoudis, E., Dziembowska, T., & Rozwadowski, Z. (1999). Photoactivation of the thermochromic solid di-anil of 2-hydroxy-5-methyl-isophthalaldehyde in β-cyclodextrin. *Journal of Photochemistry and Photobiology A: Chemistry*, *128*, 97–99. DOI: 10.1016/s1010-6030(99)00126-4.

Jafri, L., Ansari, F. L., Jamil, M., Kalsoom, S., Qureishi, S., & Mirza, B. (2012). Microwave-assisted synthesis and bioevaluation of some semicarbazones. *Chemical Biology and Drug Design*, *79*, 1–10. DOI: 10.1111/j.1747-0285.2012.01360.x.

Jia, C., Wu, B., Liang, J., Huang, X., & Yang, X. J. (2010). A colorimetric and ratiometric fluorescent chemosensor for fluoride based on proton transfer. *Journal of Fluorescence*, *20*, 291–297. DOI: 10.1007/s10895-009-0553-0.

Kang, I. J., Wang, L. W., Hsu, T. A., Yueh, A., Lee, C. C., Lee, Y. C., Chao, Y. S., Shih, S. R., Chern, J. H., & Lee, C. Y. (2011). Isatin-β-thiosemicarbazones as potent herpes simplex virus inhibitors. *Bioorganic & Medicinal Chemistry Letters*, *21*, 1948–1952. DOI: 10.1016/j.bmcl.2011.02.037.

Kolehmainen, E., Ośmiałowski, B., Nissinen, M., Kauppinen, R., & Gawinecki, R. (2000). Substituent and temperature controlled tautomerism of 2-phenacylpyridine: the hydrogen bond as a configurational lock of (*Z*)-2-(2-hydroxy-2-phenylvinyl)pyridine. *Journal of Chemical Society, Perkin Transactions 2*, *2000*, 2185–2191. DOI: 10.1039/b006879i.

Levy, D. H. (1980). Laser spectroscopy of cold gas-phase molecules. *Annual Review of Physical Chemistry*, *31*, 197–225. DOI: 10.1146/annurev.pc.31.100180.001213.

Li, Q. S., & Fang, W. H. (2003). Theoretical studies on structures and reactivity of 8-hydroxyquinoline and its one-water complex in the ground and excited states. *Chemical Physics Letters*, *367*, 637–644. DOI: 10.1016/s0009-2614(02)01791-8.

Mehata, M. S., Joshi, H. C., & Tripathi, H. B. (2002). Excited-state intermolecular proton transfer reaction of 6-hydroxyquinoline in protic polar medium. *Chemical Physics Letters*, *359*, 314–320. DOI: 10.1016/s0009-2614(02)00716-9.

Otsubo, N., Okabe, C., Mori, H., Sakota, K., Amimoto, K., Kawato, T., & Sekiya, H. (2002). Excited-state intramolecular proton transfer in photochromic jet-cooled *N*-salicylideneaniline. *Journal of Photochemistry and Photobiology A: Chemistry*, *154*, 33–39. DOI: 10.1016/s1010-6030(02)00306-4.

Pal, M., Sharma, N. K., Priynka, P., & Jha, K. K. (2011). Synthetic and biological multiplicity of isatin: A review. *Journal of Advanced Scientific Research*, *2*, 35–44.

Pandeya, S. N., Yogeeswari, P., & Stables, J. P. (2000). Synthesis and anticonvulant activity of 4-bromophenyl substituted aryl semicarbazones. *European Journal of Medicinal Chemistry*, *35*, 879–886. DOI: 10.1016/s0223-5234(00)01169-7.

Pandeya, S. N., Raja, A. S., & Stables, J. P. (2002). Synthesis of isatin semicarbazones as novel anticonvulsants – role of hydrogen bonding. *Journal of Pharmacy and Pharmaceutical Sciences*, *5*, 266–271.

Pandeya, S. N., Raja, A. S., & Nath, G. (2006). Synthesis and antimicrobial evaluation of some 4- or 6-chloroisatin derivatives. *Indian Journal of Chemistry*, *45B*, 494–499.

Sathisha, M. P., Revankar, V. K., & Pai, K. S. R. (2008). Synthesis, structure, electrochemistry, and spectral characterization of bis-isatin thiocarbohydrazone metal complexes and their antitumor activity against ehrlich ascites carcinoma in swiss albino mice. *Metal-Based Drugs*, *1*, 1–11. DOI: 10.1155/2008/362105.

Senthilkumar, L., Ghanty, T. K., & Ghosh, S. K. (2005). Electron density and energy decomposition analysis in hydrogen-bonded complexes of azabenzenes with water, acetamide, and thioacetamide. *Journal of Physical Chemistry A*, *109*, 7575–7582. DOI: 10.1021/jp052304j.

Sonawane, A. E., Pawar, Y. A., Nagle, P. S., Mahulikar, P. P., & More, D. H. (2009). Synthesis of 1,4-benzothiazine compounds containing isatin hydrazone moiety as antimicrobial agent. *Chinese Journal of Chemistry*, *27*, 2049–2054. DOI: 10.1002/cjoc.200990344.

Sridhar, S. K., Saravanan, M., & Ramesh, A. (2001). Synthesis and antibacterial screening of hydrazones, Schiff and Mannich bases of isatin derivatives. *European Journal of Medicinal Chemistry*, *36*, 615–625. DOI: 10.1016/s0223-5234(01)01255-7.

Verma, M., Pandeya, S. N., Singh, K. N., & Stables, J. P. (2004). Anticonvulsant activity of Schiff bases of isatin derivatives. *Acta Pharmaceutica*, *54*, 49–56.

Verma, K., Pandeya, S. N., Singh, U. K., Gupta, S., Prashant, P., & Anurag Gautam, B. (2009). Synthesis and pharmacological activity of some substituted menthone semicarbazone and thiosemicarbazone derivatives. *International Journal of Pharmaceutical Sciences and Nanotechnology*, *1*, 357–362.

Wu, D. L., Liu, L., Liu, G. F., & Jia, D. Z. (2007). Theoretical studies on geometrical properties and photochromic mechanism of two photochromic compounds. *Journal of Molecular Structure: THEOCHEM*, *806*, 197–203. DOI: 10.1016/j.theochem.2006.11.027.

Zhao, Y., & Truhlar, D. G. (2008). The M06 suite of density functionals for main group thermochemistry, thermochemical kinetics, noncovalent interactions, excited states, and transition elements: two new functionals and systematic testing of four M06-class functionals and 12 other functionals. *Theoretical Chemistry Accounts: Theory, Computation, and Modeling (Theoretica Chimica Acta)*, *120*, 215–241. DOI: 10.1007/s00214-007-0310-x.